Journal of Neurochemistry JNC

# Altered cerebrovascular reactivity in reduced cerebral perfusion in rats with acute liver failure: the role of L-glutamine and asymmetric dimethylarginine in L-arginine-induced response



| | |
|---|---|
| Journal: | *Journal of Neurochemistry* |
| Manuscript ID | JNC-2018-0329 |
| Manuscript Type: | Original Article |
| Date Submitted by the Author: | 06-Jun-2018 |
| Complete List of Authors: | Czarnecka, Anna; Mossakowski Medical Research Centre, Neurotoxicology<br>Aleksandrowicz, Marta; Mossakowski Medical Research Centre, Neurosurgery<br>Jasiński, Krzysztof; Institute of Nuclear Physics, Polish Academy of Sciences, Magnetic Resonance Imaging<br>Jaźwiec, Radosław; Institute of Biochemistry and Biophysics, Polish Academy of Sciences, Mass Spectrometry Laboratory<br>Kalita, Katarzyna; Institute of Nuclear Physics, Polish Academy of Sciences, Magnetic Resonance Imaging<br>Hilgier, Wojciech; Mossakowski Medical Research Centre, Neurotoxicology<br>Zielińska, Magdalena; Mossakowski Medical Research Centre, Neurotoxicology |
| Area/Section: | Molecular Basis of Disease |
| Keywords: | Acute liver failure, asymmetric dimethylarginine, cerebral blood flow, isolated middle cerebral artery, MRI-ASL |
| | |

# Altered cerebrovascular reactivity in reduced cerebral perfusion in rats with acute liver failure: the role of L-glutamine and asymmetric dimethylarginine in L-arginine-induced response

Anna Czarnecka[1], Marta Aleksandrowicz[2], Krzysztof Jasiński[3], Radosław Jaźwiec[4], Katarzyna Kalita[3], Wojciech Hilgier[1], Magdalena Zielińska[1]

[1]*Department of Neurotoxicology, Mossakowski Medical Research Centre, Polish Academy of Sciences, 5 Pawińskiego Street, 02-106 Warsaw, Poland.*
[2]*Department of Neurosurgery, Mossakowski Medical Research Centre, Polish Academy of Sciences, 5 Pawińskiego Street, 02-106 Warsaw, Poland.*
[3]*Department of Magnetic Resonance Imaging, Institute of Nuclear Physics, Polish Academy of Sciences, Kraków, Poland.*
[4]*Mass Spectrometry Laboratory, Institute of Biochemistry and Biophysics, Polish Academy of Sciences, 5A Pawińskiego Street, 02-106 Warsaw, Poland.*

Keywords

Acute liver failure, asymmetric dimethylarginine, cerebral blood flow, isolated middle cerebral artery, MRI-ASL

Abstract

Cerebral blood flow (CBF) is impaired in acute liver failure (ALF) and the results are often inconclusive due to complexity of the underlying mechanism. Regulation of CBF depends at least partially on variations in the local brain L-arginine concentration and/or its metabolic rate. In ALF, other factors, like an increased concentration of asymmetric dimethylarginine (ADMA), an endogenous nitric oxide synthase inhibitor and elevated level of L-glutamine, may contribute to CBF alteration. The present study demonstrated strong differences in the reactivity of the middle cerebral arteries and their response to extravascular L-arginine application between vessels isolated from rats with thioacetamide (TAA)-induced ALF and control animals. Our results also showed the decrease in the cerebral perfusion in TAA rats measured by arterial spin labeling perfusion magnetic resonance. Subsequently, we aimed to investigate the importance of balance between the concentration of ADMA and L-arginine in the CBF regulation. *In vivo*, intraperitoneal L-arginine administration in TAA rats corrected: i) decrease in cerebral perfusion, ii) decrease in brain extracellular L-arginine/ADMA ratio and iii) increase of brain L-glutamine concentration. Our study implicates that impaired vascular tone of cerebral arteries is most likely associated with sustained exposure to high ADMA and L-glutamine levels resulting in limited availability of L-arginine and might be responsible for reduced cerebral perfusion observed in ALF.

## Introduction

The accumulation of neurotoxic substances in the brain, due to acute or chronic liver failure (ALF vs. CLF), results in neurological alterations known as hepatic encephalopathy (HE) (Butterworth 2003; Felipo 2013). The pathomechanism of HE remains complex, however, the general consensus is that neurotoxic effects of blood-derived ammonia in the brain compounded by central and systemic inflammatory processes play a dominant role (Butterworth 2013; Liere *et al.* 2017). It is generally assumed that intra-astrocytic accumulation of glutamine, a product of ammonia detoxification *via* enzymatic conversion of glutamate by glutamine synthetase (Norenberg and Martinez-Hernandez 1979), directly contributes to brain edema and other clinical manifestations of HE (Butterworth 2013; Albrecht *et al.* 2010).

Neurological dysfunctions accompanying HE progression may result from low cerebral oxygen metabolism which is the primary event contributing to dysregulation of cerebral blood flow (CBF) (Felipo 2013; Iversen *et al.* 2009; Iversen *et al.* 2014; Zheng *et al.* 2012). Importantly, CBF alteration related to endothelial dysfunction associated with nitric oxide (NO) signaling is relatively less examined aspect of HE pathology (Palenzuela *et al.* 2016). Depending on etiology and time point in disease progression, cerebral perfusion has been found both increased or decreased (Iversen *et al.* 2009; Zheng *et al.* 2012; Jalan *et al.* 2004). This discrepancy raises difficulties in the choice of treatment strategy. Importantly, regional CBF differences were also observed[2], however, an explanation of this phenomenon is not known.

CBF, which has the potential of being used as the indicator of brain dysfunction (Becker *et al.* 1996; Iversen *et al.* 2009), is related to L-arginine metabolism, therefore, synthesized and/or released nitric oxide (NO) is arguably the most important endogenous vasodilator in the regulation of cerebral perfusion (Keynes and Garthwaite 2004). Asymmetric dimethylarginine (ADMA), an endogenous inhibitor of NO synthesis, is present in a relatively high concentration in the brain (Teerlink *et al.* 2009). Thus, one of physiological effects of ADMA might be to control the cerebrovascular reactivity and CBF in resting conditions. Since elevated ADMA concentrations were frequently documented in patients with HE and animal models of HE, as reviewed by Czarnecka et al. (Czarnecka *et al.* 2017), a direct response of HE-affected vessels and a possible role of ADMA in CBF regulation in this pathology, have to our knowledge never been assessed. Importantly in this context, topical application of

ADMA in the rat brain constricted the basilar artery (Faraci *et al.* 1995). In turn, exogenously added ADMA caused concentration- and endothelium-dependent contraction of the human middle cerebral artery (MCA) (Segarra *et al.* 1999) which was prevented by L-arginine (Chen *et al.* 2012). L-arginine was reported to improve vascular function by overcoming deleterious effect of ADMA (Böger and Ron 2005). Furthermore, systemic administration of L-arginine exerted a beneficial effect on the cortical CBF in the experimental stroke (Willmot *et al.* 2005) and brain trauma (Lundblad and Bentzer 2007).

L-arginine availability for NO synthesis in the brain may be regulated by elevated concentration of glutamine (Kawaguchi *et al.* 2005). Previously reported data indicated that L-glutamine acted by inhibition the L-citrulline to L-arginine recycling, thereby limiting L-arginine availability for NO production. In support of this concept, an excess of L-arginine overcame the inhibitory effect of L-glutamine on vascular reactivity as demonstrated *in vivo* (Okada *et al.* 2000). In addition, pharmacologically increased extracellular L-glutamine in the brain reduced NO and subsequently cGMP production both, in healthy and ammonia-exposed rat brain (Hilgier *et al.* 2009). Accordingly, pre-incubation with L-glutamine stimulated L-arginine efflux from rat brain slices (Zielińska *et al.* 2011) *via* a mechanism involving y+L transport system (Zielińska *et al.* 2012; 2015).

In the present study we compared the basal reactivity of isolated MCAs and cerebral perfusion of control and ALF rats. The MCA was chosen for this study because as a resistance vessel it participates in the regulation of cerebral blood flow (Faraci and Heistad 1990). The analyses were conducted in a well-established rat model of ALF induced by intraperitoneal administration of the hepatotoxin, thioacetamide (TAA), which reproduces most of the cerebral metabolic changes and symptoms observed during ALF. Importantly, the elevated concentration of ADMA and L-glutamine in the brain and plasma of TAA rats have been previously documented (Hilgier *et al.* 1994; 1996; Czarnecka *et al.* 2017; Milewski *et al.* 2015; 2017).

Therefore, the specific aims of this study were to investigate in the TAA-induced rat model of ALF: (i) vasodilatory status and reactivity of the isolated MCAs to extravascular L-arginine; (ii) extracellular brain concentration of amino acids and ADMA after ip infusion of L-arginine; (iii) CBF changes induced by ip administration of L-arginine.

Materials and methods

***Animals***

The studies were conducted on 36 male Sprague–Dawley rats, animal colony supplied by the Animal House of Mossakowski Medical Research Centre, Warsaw, Poland of initial body weight from 220 to 275 g kept 2-3 under standard laboratory conditions in cages model 1291H Eurostandard Type III H at room temperature (22$^{o}$ C) under an artificial light/dark cycle (12/12 h), with free access to standard laboratory food and tap water. All procedures were conducted in accordance with the National Institutes of Health Guidelines for the Care and Use of Laboratory Animals, and received a prior approval from the Bioethics Commission of the Academy, as compliant with Polish Law (of January 21, 2005). The experimental procedures were approved by the 4$^{th}$ Local Ethics Committee for Animal Experimentation, Warsaw, Poland. All efforts were made to reduce the number of animals and to minimize their suffering. The study complies with the ARRIVE guidelines for reporting animal research. All procedures on animals were carried out in a randomized manner. This study was not pre-registered.

***Study design and animal groups***

Animals were randomly divided into two experimental groups: control (16 rats) and acute liver failure (20 rats). All further experiments were performed 72 hours after the last thioacetamide (TAA)/saline dose. Isolated cerebral artery studies were conducted on 5 control and 8 TAA rats, microdialysis study was carried out on 5 control and 5 TAA rats and ASL-MRI perfusion measurement on 6 control and 7 TAA rats, respectively.

Number of animals was determined based on pilot studies which provided statistically significant differences between test and control.

***Acute liver failure model***

HE was induced by three intraperitoneal (ip) injections of TAA (Sigma-Aldrich, Steinheim, Germany) (300 mg/kg body weight.) at 24 h intervals (Hilgier and Olson 1994). Control rats were administered i.p. with saline solution according to the analogical scheme.

***Isolated cerebral artery studies***

Middle cerebral arteries (MCAs) were isolated from the brain of control and TAA rats and located in an organ chamber filled with physiological saline solution buffered with MOPS (3-(N-morpholino) propanesulfonic acid), (MOPS-PSS) with 1% dialyzed bovine serum albumin (BSA) addition (pH 7.4 adjusted by NaOH), as it was described in detail previously (Aleksandrowicz *et al.* 2017). The organ chamber was placed at the stage of inverted microscope (CKX41, Olympus, Germany) connected with a video camera and a monitor for analysis of inner diameters of the arteries. The vessels were perfused with MOPS-PSS containing 1% BSA at a transmural pressure of 80 mm Hg. Extraluminal fluid was switched to MOPS-PSS without BSA, heated to 37°C using a water bath and the medium was exchanged at a rate of 20 mL/min with the help of a peristaltic pump (Masterflex, Cole Parmer, USA). After developing myogenic tone, i.e. a contraction by about 30% - 40% of the initial diameter, smooth muscle cell function was tested by increasing extraluminal $K^+$ ion concentration from 3 mM to 20 mM. MCAs which did not develop myogenic tone were excluded from further studies.

The responses of the isolated, cannulated and pressurized MCAs to extravascular administration of L-arginine (100 μM) were assessed after 20 min of continuous perfusion in few variants. The dose of L-arginine was chosen based on the available literature (Kajita *et al.* 1995; Tsikas *et al.* 2000). The arteries from control (untreated with TAA) rats were studied: (a) in the standard MOPS - PSS containing: 3.0 mM MOPS, 145.0 mM NaCl, 3.0 mM KCl, 2.5 mM $CaCl_2$, 1.5 mM $MgSO_4$, 1.21 mM $NaH_2PO_4$, 0.02 mM EDTA, 2.0 mM sodium puryvate, 5.0 mM glucose, or (b) MOPS-PSS + 400 μM $NH_4Cl$. The MCAs isolated from TAA rats were maintained depending on the experimental variant in the presence of ammonium ions and ADMA at concentration equal to those observed in plasma *in vivo*, therefore, the following groups were studied: (c) MOPS-PSS + 400 μM $NH_4Cl$, or (d) MOPS-PSS + 400 μM $NH_4Cl$ + 1 μM ADMA, or (e) MOPS-PSS + 400 μM $NH_4Cl$ + 2 μM ADMA. The dose of ammonia and ADMA, respectively, were chosen based on the data reporting concentrations of these substances in plasma of TAA rats (Milewski *et. al.* 2015; Milewski 2017).

At the end of the experiment, maximal dilation of the vessel was obtained in calcium-free MOPS-PSS containing EGTA (3 mM). Percent response of the MCA to L-arginine was calculated using the formula: $(D_{active} - D_{baseline})/(D_{maximum} - D_{baseline})*100\%$, where $D_{active}$ is the diameter obtained after L-arginine administration, $D_{baseline}$ is the diameter prior to application of L-arginine, and $D_{maximum}$ is the diameter in calcium-free MOPS-PSS with EGTA. Percent

tone was calculated as a percent decrease in diameter from the initial diameter measured directly after pressurizing. All reagents used in these experiments were purchased from Sigma-Aldrich.

***Microdialysis of the rat prefrontal cortex***

Bilateral microdialysis of the prefrontal cortex was performed 24 h after the last TAA administration as described previously (Czarnecka *et al.* 2017). The rats were anesthetized with 5% isoflurane (Baxter, Warsaw, Poland) in air within 2 min and then anesthesia was maintained during the whole experiment with a 2% isoflurane-air mixture. The body temperature was kept at 37.3$^{o}$C by a heating pad controlled by a rectal thermometer. The animals were fixed in a Stoelting stereotaxic frame. Briefly, concentric microdialysis probes (dialyzing membrane: diameter 0.5 mm; length 3 mm, CMA 12 Elite, CMA Microdialysis, Stockholm, Sweden) were implanted bilaterally into the prefrontal cerebral cortex through a small hole drilled in the skull (stereotaxic coordinates according to the atlas of Paxinos and Watson[37] were as follow: A/P + 3.0; L +(-) 1.0; D/V -3.5). The probes were perfused with artificial cerebrospinal fluid (aCSF), pH 7.4, containing: 126 mM NaCl, 2.4 mM KCl, 1.1 mM $CaCl_2$, 0.8 mM $MgCl_2$, 0.5 mM $KH_2PO_4$, 6 mM glucose (PoCH, Gliwice, Poland) at a rate of 2.5 µl/min. Six fractions were collected every 40 min (0-240 min), starting 30 min after implantation of the probe. L-arginine (200 mg/kg/3 ml) (Sigma-Aldrich, Steinheim, Germany) was injected ip to the anesthetized rat immediately after collecting 2$^{nd}$ fraction (110 min after implantation of the probe). The dose of L-arginine was chosen based on the data reporting the effective doses for stimulation of regional cerebral blood flow (Morikawa *et al.* 1992) and preliminary studies which demonstrated that ip injection of 200 mg/kg of L-arginine resulted in the increased brain extracellular L-arginine concentration up to 5-10 µM. Taking into account average *in vitro* recovery of CMA probes at 15 %, this dose of L-arginine increased brain extracellular level to ~100 µM similarly to concentration used in *ex vivo* vascular experiments. After completion of the microdialysis, the anesthetized rats were immediately sacrificed by decapitation. Dialysates were stored at -80 ºC until further procedures were applied. The researchers analyzing samples were entirely blinded to the experimental groups.

***Positive mode electrospray LC–DMS–MS/MS***

HPLC grade ethanol (EtOH), HPLC grade formic acid, gradient grade acetonitryle (ACN), LC/MS grade ACN from J.T. Baker (Deventer, The Netherlands) were purchased from

Witko. MQ Water was purified with Millipore (Millipore, Bedford, MA, USA) MiliQ instrument.

The extracellular levels of ADMA and L-arginine (ARG) were analyzed using positive mode electrospray LC–DMS–MS/MS as described previously (Czarnecka *et al.* 2017) with a slight modification. The sample (20 µl) was mixed with 80 µl of ADMA-D6 and ARG D5 (IS) (Sigma-Aldrich, Steinheim, Germany) solution in EtOH (4 ng/ml and 100 ng/ml, respectively). The solution was evaporated to dryness under nitrogen, reconstituted with 45 µl of acetonitryle (ACN) and transferred to chromatographic vials. Calibration curve was prepared using the same buffer as for microdialysis. Eight calibration points were prepared in the range from 0.55 ng/ml to 40.7 ng/ml for ADMA, and from 0.12 µg/ml to 3.157 µg/ml for ARG. Samples were analyzed using Waters Xevo TQ-S triple quadrupole mass spectrometer coupled with Waters Acquity I-Class UPLC. A 3 min HPLC method was set up on Waters HILIC equipped with 1.7 µm 2.1 x 100 mm column with thermostatic control at 70$^{o}$C. Mobile phase A was composed of 0.025% (trifluoroacetic acid) TFA + 1% acetic acid (AA) in ACN, mobile phase B: 0.025% TFA + 1% AA in MQ. Linear gradient from 7% to 25% of phase B was used within 2.0 min with the flow rate of 0.65 ml/min. Injection volume was 3 µl. Retention time for ADMA was 1.62 min, for ARG 1.67 min. MS detector worked with ESI ionization source in MRM mode. Separation was initiated with setting up MRM transitions that were highly specific for each compound. Using transitions 203.15 > 46.11 (collision energy 14) for ADMA we saw no crosstalk between signals of both compounds as it was previously reported in literature (Martens-Lobenhoffer *et al.* 2012; Zotti *et al.* 2008). Monitored transmission for ADMA-D6 (IS) was 209.19 > 164.19 (collision energy 15). Monitored transmission for ARG was 175.12 > 70.03 (collision energy 7) and for ARG-D5 (IS) was 180.12 > 75.07 (collision energy 55). Collision energies for ARG and ARG-D5 were set up not for optimal sensitivity, since concentration of ARG in CSF is high and very good sensitivity is not needed. They were optimized to eliminate crosstalk from ARG to ADMA and increase linear range of method for ARG. MS parameters were: Capillary (kV) 3.00; Cone (V) 30.00; Source Offset (V) 40.0; Source Temperature (°C) 150; Desolvation Temperature (°C) 550; Cone Gas Flow (L/Hr - Nitrogen) 150; Desolvation Gas Flow (L/Hr - Nitrogen) 1000; Collision Gas Flow (mL/Min) 0.15; Nebuliser Gas Flow (Bar) 7.00.

***Glutamine determination in microdialysates***

Glutamine was assayed in microdialysate samples using HPLC with fluorescence detection after derivatization in a timed reaction with o-phthalaldehyde plus mercaptoethanol (Kilpatrick *et al.* 1991). The derivatized samples (50 µl) were injected onto a 150 × 4.6 mm, 5 µm Hypersil ODS column with a mobile phase composed of 50 mM phosphate buffer ($KH_2PO_4$ / $K_2HPO_4$) containing 10% v/v methanol, pH 6.2 (solvent A), and methanol (solvent B). The methanol gradient was 20–70 % and the elution time was 20 min. The obtained values of extracellular neurotransmitter levels were not corrected for *in vitro* probe recovery.

***Arterial Spin Labeling (ASL) MRI***

The MRI (Magnetic Resonance Imaging) was conducted using a 9.4T horizontal scanner (BioSpec 94/20 USR, Bruker, Ettlingen, Germany) equipped with BGA6S gradient system. Images were acquired using 86 mm internal diameter birdcage RF coil (Bruker T12054V3) used for transmission while rat brain receive-only circularly polarized surface coil with integrated preamplifier and combiner used for signal reception (Bruker T11207V3). Perfusion measurement was performed 24 hours after the last dose of TAA or saline. An induction chamber with 2% isoflurane (Baxter, Poland) was used for anesthesia induction. During MRI isoflurane anesthesia was delivered via nosecone and maintained at 1.7% in a 1:2 oxygen/air mixture. Animal body temperature was maintained at 37°C using temperature controlled warming pad. Physiological parameters: ECG, respiration and body temperature were monitored with Monitoring and Gating System Model 1025 (SA Instruments Inc., Stony Brook, NY, USA). The animals were placed prone in the cradle throughout the imaging sessions lasting 2-2.5 hours with head stabilized using three point-fixation system (tooth-bar and ear plugs). Before the imaging 2 ml of saline was injected subcutaneously to prevent dehydration. Bolus injection of L-arginine (200 mg/kg/3ml) at a concentration capable of increasing brain L-arginine level as tested in microdialysis experiment, was delivered in the scanner with the use of an intraperitoneally placed cannula. Based on scout images two slice positions in the prefrontal cortex and cerebellum were selected for perfusion measurement. An exemplary location of these slices is shown in Fig. 5a. The measurements of the cerebral perfusion were performed in the following sequence: baseline assessment (pre) prefrontal cortex slice (24 min), cerebellum slice (24 min), L-arginine ip injection, 30 min interval and again prefrontal cortex slice (24 min), cerebellum slice (24 min) (post L-arginine) in the same geometry as the baseline. Immediately after MRI measurements, each rat received a lethal dose of pentobarbital (Biowet, Poland).

For tissue perfusion and $T_1$ relaxation time measurement respiratory-gated FAIR-RARE (Flow-sensitive Alternating Inversion Recovery) sequence with the following parameters was used: repetition time (TR) 10000ms, echo time (TE) 5.1ms, number of averages (NA) 4, Rare Factor 72, field of view (FOV) 27x27mm, acquisition matrix (MTX) 128x128, resolution 211x211μm, slice thickness 1.5mm, 14 inversion times (TI) ranging from 30 to 3000 ms, acquisition time 24min (approximately).

Quantitative calculations of perfusion were performed with in-house written Matlab (The MathWorks Inc., Natick, MA, U.S.A.) script. In order to minimize possible fitting artifacts related to animal movement during a quite long measurement causing corresponding pixel shift on consecutive images with different TI, rigid transformation with Matlab imregister function was used to align all images within one scan to the first image in this scan. Then pre and post L-arg scans were aligned (second to first) as well. $T_1$ relaxation time parametric maps were calculated pixel by pixel fitting inversion curve with Matlab nonlinear least-squares solver function lsqcurvefit for the area (ROI) covering the brain, drawn by hand for each animal. Examples of such areas for prefrontal cortex and cerebellum slices, marked with yellow line on anatomic images are shown in Figure MRI2 (first and fourth column). Then blood flow maps were calculated according to Belle et al. (Belle *et al.* 1998) The examples of the perfusion maps are presented in Fig. 5c. Finally to get perfusion value for each animal in the prefrontal cortex and cerebellum, perfusion values were averaged from manually drawn ROIs shown in Fig. 5b. One rat from the TAA treated group was excluded from the calculations because it died during the magnetic resonance procedure.

***Statistical analysis***

All experiments were carried out with replicates in terms of animals per group as indicated. No test for outliers was conducted on the data obtained in the study. Data were tested for normal distribution with a Shapiro-Wilk test. Since they were normally distributed, a one-way or a repeated measures ANOVA with the post hoc Newman-Keuls or Tukey was performed. The data are presented as the mean ± standard error of the mean (mean ± SEM). A significance level of $p < 0.05$ was chosen for all tests. All statistical analyses were performed using the Statistica software package (Statsoft Inc., USA) and GraphPad Prism 7 (GraphPad Software, Inc., USA).

Results

***Isolated cerebral artery studies***

***The effect of ADMA on the baseline MCA reactivity***

Incubation of MCAs from TAA rats in MOPS buffer containing ADMA at a dose of 2 μM resulted in a smaller initial vessel diameter measured directly after pressurizing (~78% of the control value, $p<0.05$ vs. Control+$NH_4$ group), greater spontaneous myogenic tone development after 1 h stabilization (51%, $p<0.001$ vs. 33% in the control group) and higher vessel dilation in response to 20 mM KCl challenge (91%, $p<0.01$ vs. 43% in the control group) (Fig. 1 a-c). Moreover, a decreasing tendency in vessel diameter as well as increasing tendency to greater myogenic tone development and vessel dilation in response to 20 mM KCl were observed at the lower ADMA dose (1 μM) when compared to the control group (Fig. 1 a-c).

***The effect of extravascular administration of L-arginine on MCA diameter***

Extraluminal administration of L-arginine at a concentration of 100 μM resulted in a dilation of the MCA derived from TAA rats. The dose of 100 μM elicited a comparable vasodilation of the MCA in all TAA groups (~55 % of the maximum diameter, $p < 0.01$; Fig. 2).

***The effect of systemic administration of L-arginine on cortical extracellular levels of L-arginine and ADMA***

Administration of TAA (300 mg/kg/ip) resulted in a significant increase in extracellular ADMA concentration (to 260%, $p < 0.01$). The intraperitoneal injection of L-arginine (200 mg/kg/3ml) did not significantly affect ADMA concentration both in control and TAA rats (Fig. 3a). The ANOVA for repeated measures revealed significant effects of treatment ($F_{1,8} = 9.70$, $p < 0.05$).

The intraperitoneal injection of L-arginine (200 mg/kg/3ml) resulted in a significant increase in cortical L-arginine level in TAA rats (to 185%, $p < 0.001$, Fig. 3b). The ANOVA for repeated measures revealed significant effects of treatment, time and treatment × time interaction ($F_{1,8} = 8.03$, $p < 0.05$; $F_{3,24} = 9.63$, $p < 0.001$, $F_{3,24} = 5.29$, $p < 0.01$, respectively).

The L-arginine/ADMA ratio was significantly decreased in TAA rats (to 68%, $p < 0.05$, Fig. 3c). L-arginine administration increased this ratio to the level in the control group. The ANOVA for repeated measures revealed a significant effects of time ($F_{3,24} = 6.44$, $p < 0.01$).

***The effect of exogenous L-arginine on extracellular glutamine level in the prefrontal cortex of ALF rats***

Basal extracellular level of glutamine was significantly increased in the prefrontal cortex of TAA rats (~215 % of the control level). L-arginine (200 mg/kg/ip) significantly decreased extracellular glutamine (71% of the basal TAA level) as measured 120 min after injection (Fig. 4). Repeated measures ANOVA revealed a significant effect of group and L-arginine ($F_{1,8} = 13.35$ $p < 0.01$, $F_{1,8} = 12.40$ $p < 0.01$, respectively).

***Assessment of perfusion with arterial spin labeling: the effect of L-arginine***

Perfusion in the prefrontal cortex ROIs (Fig. 5b, yellow circles) was equal to 82 ± 5 ml/min/100 g in the control group and decreased to 58 ± 5 ml/min/100 g in the TAA group. L-arginine injection resulted in the increase in perfusion to 98 ± 7 ml/min/100 g in the control group and 66 ± 4 ml/min/100 g in the TAA group (Fig. 5d). Repeated measures ANOVA revealed significant effects of group and L-arginine stimulation ($F_{1,10} = 15.44$ $p < 0.01$; $F_{1,10} =$ 22,76, $p < 0.001$, respectively).

Perfusion in the cerebellum ROIs (Fig. 5b, red circle) was equal to 133 ± 7 ml/min/100 g in the control group and decreased to 85 ± 5 ml/min/100 g in the TAA group. L-arginine injection increased perfusion to 100 ± 9 ml/min/100 g only in the TAA group (Fig. 5e). Repeated measures ANOVA revealed significant effects of group and L-arginine stimulation and group x L-arginine interaction ($F_{1,10} = 15.75$ $p < 0.01$; $F_{1,10} = 5.88$ , $p < 0.05$, $F_{1,10} = 13.61$, $p < 0.01$, respectively).

## Discussion

The present study demonstrates, to our knowledge for the first time, the reduced initial vessel diameter and impaired reactivity of pressurized middle cerebral arteries (MCAs) isolated from rats with thioacetamide (TAA)-induced acute liver failure (ALF), which supports ADMA contribution to the cerebral blood flow (CBF) decrease. Other new findings of the study include demonstration that (i) exogenous L-arginine application resulted in the excessive dilatation of MCAs from TAA rats *ex vivo*, (ii) intraperitoneal administration of L-arginine partially reversed the reduction of cerebral blood flow (CBF) in the cerebral cortex and cerebellum of TAA rats, and (iii) administration of L-arginine corrected the cerebral L-arginine/ADMA ratio and decreased extracellular glutamine. These aspects deserve further comments.

The MCA are a widely accepted tool for measurement of brain vascularity response to various stimuli (Faraci and Heistad 1990). What is important, the use of isolated vessels eliminates parenchymal influences and slow perfusion of the vessel while pressurization to the physiological level of blood pressure simulates *in vivo* conditions, and ensures proper myogenic tone and shear stress. MCAs from TAA rat brain were maintained in the environment that reproduced the status of vessels *in vivo* and contained pathophysiological concentration of ammonium ions and ADMA (equal to the plasma concentration in TAA rats, Milewski *et al.* 2015). TAA vessels manifested a smaller initial vessel diameter, higher myogenic tone and larger vasodilation in viability test as compared to the vessels isolated from control rats. It may be assumed that smaller basal diameter of vessels incubated with 2 μM ADMA resulted in their greater vasodilatory reserve and therefore greater response to K+ test. Previously, it was reported that concentration of ADMA that inhibited activity of brain NO synthase by 50 % in the cerebrum and cerebellum was approximately 2 μM (Faraci *et al.* 1995). It is consistent with the present study showing that MCAs developed the increase in vascular tone in the presence of pathophysiologically elevated ADMA. Topical application of ADMA through cranial windows to rats constricted the basilar artery (BA) (Faraci *et al.* 1995), whereas exogenously perfused ADMA evoked concentration- and endothelium-dependent contractions of the human middle cerebral artery (Segarra *et al.* 1999). Consequently, exogenous ADMA-induced contraction of human middle cerebral artery rings was prevented by L-arginine (Chen *et al.* 2012).

In our study MCAs isolated from control and TAA rats responded differently to exogenous L-arginine application. Vessels isolated from TAA rats dilated by more than 50% of its maximum diameter as opposed to control MCAs which did not respond to L-arginine. This somewhat surprising result requires a detailed explanation.

Studies reporting changes in the concentration of plasma L-arginine in ALF are not conclusive. Some reports found either unchanged (Tietge *et al.* 2002), reduced (Yagnik *et al.* 2002) or increased (Cardounel *et al.* 2007) plasma L-arginine values. Furthermore, an increased level of plasma arginase during liver failure (Das *et al.* 2008) can additionally reduce the amount of available arginine, reducing endothelial NOS-mediated NO synthesis. In the TAA model, used in this study, plasma level of L-arginine was significantly decreased (Milewski 2017), which may provide a potential explanation of the above observation as masking of the effect of supplementation.

The so far available data describing the effect of L-arginine on the cerebral blood vessels reactivity are also variable. L-arginine did not affect the diameter of intra-parenchymal arterioles (Kimura *et al.* 1994), MCAs (Kovách *et al.* 1992) and BA (Rossitch *et al.* 1991) *in vitro* and had no effect on BA resistance (Faraci 1990) and CBF measured *in vivo* (Kovách *et al.* 1992; Faraci and Heistad 1992). In contrast, Rosenblum et al. (Rosenblum et al. 1990) and Morikawa et al. (Morikawa et al. 1992) reported a dilation of pial arterioles in response to L-arginine *in vivo* and Kajita et al. (Kajita et al. 1995) observed dilation of the MCA, BA and anterior cerebral artery *in vivo* and parenchymal arterioles *in vitro*. In our study 100 μM dose of L-arginine did not exert vasodilator response in control MCAs, while the response of those derived from TAA rats was substantial. Lack of the relaxation of the MCAs from control rats in response to L-arginine indicates that L-arginine is not rate-limiting for NOS activity, in contrast to its strong vasodilatory effect observed in MCAs isolated from TAA rats. It seems that the rate-limiting effect of L-arginine for NO synthesis may be due to the increased plasma ADMA and/or cellular uptake of L-arginine in TAA model. The later possibility is reasonable, since a significant increase in [$^3$H]citrulline, a direct L-arginine precursor for *de novo* NO synthesis, into TAA cortical slices was previously reported (Zielińska *et al.* 2014). The former possibility deserves a comment. The increased L-[H$^3$]arginine uptake have been reported in ammonium acetate-affected cerebellar synaptosomes (Rao *et al.* 1997) and synaptosomal preparations from TAA rats (Albrecht *et al.* 1990). MCAs isolated from control rats did not relax in response to L-arginine in the presence

of ammonium ions indicating that short-lasting hyperammonemia has a slight impact on the rate-limiting effect of L-arginine for NO synthesis.

L-arginine may elevate NO production by increasing the substrate availability. However, its levels in plasma and cells are considerably higher than the eNOS $K_m$ for L-arginine (Arnal *et al.* 1995; Harrison 1997). The fact that L-arginine drives NO production even when intracellular L-arginine levels are in excess is called the "arginine paradox" (Arnal *et al.* 1995; Harrison 1997; Böger and Ron 2005; Bode-Böger *et al.* 2007). It is assumed that in the presence of pathologically relevant concentrations of ADMA and physiological concentration of L-arginine, the endothelial NOS activity decreases, which results in NO formation rates below the physiological level. Therefore, in these conditions, supplementation of exogenous L-arginine competes with its inhibitor and restores the physiological L-arginine/ADMA ratio (Bode-Boger *et al.* 2007). Thus, it appears that L-arginine may become a rate-limiting factor for NO synthesis in clinical conditions, but not in healthy individuals. Clinical and experimental evidence suggests that elevation of ADMA can cause a relative L-arginine deficiency, even in the presence of physiological L-arginine levels. As ADMA is a competitive inhibitor of eNOS, its inhibitory action can be overcome by increasing the concentration of the enzyme's substrate, L-arginine (Böger and Ron 2005).

However, in the present study, response of TAA-exposed vessels to 100 μM L-arginine was independent of the short-term incubation with pathological concentration of ADMA. Strong vasodilation of MCAs in response to L-arginine was a common feature of all TAA rats independently of ADMA concentration in the buffer. One cannot exclude, however, that, to some extent, three-day exposure to elevated endogenous ADMA concentrations resulted in a prolonged substrate (L-arginine) deficiency and higher sensitivity of eNOS enzyme in brain vessels. The potential influence of ADMA presence in the buffer was probably masked by the enormous contractile response of TAA MCAs to exogenous L-arginine.

On the other hand, ADMA is not the only factor explaining the pronounced reactivity of TAA vessels in response to L-arginine. Aside from the L-arginine/ADMA balance, glutamine might be an important factor in the regulation of vascular response in HE condition. *In vitro* evidence in endothelial cells and perivascular nerves indicated that glutamine inhibited recycling of L-citrulline to L-arginine, thereby limiting L-arginine availability for NO production (Chen and Lee 1995; Lee *et al.* 1996). The mechanism of L-glutamine action

involves inhibition of argininosuccinate synthetase, an enzyme that is a part of the two-step recycling of L-citrulline to L-arginine for use by NOS (Sessa *et al.* 1990). Hyperammonemia, accompanying liver diseases is one of the pathophysiological conditions in which L-glutamine level increases (Cooper and Plum 1987). The increase in L-glutamine is prominent in ALF brain where glia cells are enriched in glutamine synthetase. The CBF response to hypercapnia is abolished during acute hyperammonemia (Durham *et al.* 1995; Takahashi *et al.* 1992). Inhibition of glutamine synthetase during hyperammonemia preserved the CBF (Takahashi *et al.* 1992) and pial arteriolar response to $CO_2$ (Hirata *et al.* 1999) indicating that the impaired response was related to glutamine synthesis rather than to the increased concentration of ammonium ions. Glutamine presumably acts by limiting arginine availability because the vascular inhibitory effect required a few hours to develop and arginine infusion counteracted the vascular effect produced by the increased glutamine (Okada *et al.* 2000). Arnal et al. (Arnal *et al.* 1995) reported that L-arginine reversed L-glutamine's ability to inhibit NO release in bovine aortic endothelial cells and in rabbit aortic rings. In their study, L-arginine dose dependently enhanced the endothelium-dependent vascular relaxation only when L-glutamine was present, suggesting a complex interplay between L-glutamine and receptor-mediated activation of NO synthase. Moreover, this paradox may be influenced by endogenous NO synthase antagonists, such as ADMA (Harrison 1997). The present results indicated that extracellular concentration of L-glutamine was highly increased in the cerebral cortex of TAA rats while intraperitoneal injection of L-arginine significantly decreased it. It confirms that glutamine-induced vascular impairment may be overcome by the addition of exogenous L-arginine.

Vascular reactivity is dependent on signals originating both from neurons and from astrocytes. Importantly, astrocytes contribute to the fine-tune regulation of cerebral vascular tone and CBF by producing and releasing both vasodilatory and vasoconstrictive compounds (Filosa *et al.* 2016). In addition, spatial regulation of astrocyte-induced dilations and constrictions contributing to the CBF changes were observed during fMRI recordings of brain activity (Metea and Newman 2006). The increased glutamine synthesis, beyond being the origin of astrocytic impairment under ALF state (Albrecht *et al.* 2017), might also impair neurovascular coupling as such. Thus, the balance of astrocyte-derived glutamine may contribute to the fine-tune regulation of cerebral vascular tone and CBF in ALF as well, however, more detailed studies are required.

We can suppose that the consequences of high ADMA brain concentration included the reduction of CBF both in the cerebral cortex and cerebellum, demonstrated in TAA rats. A significant impact of ADMA on CBF regulation under resting and pathologically changed conditions by NOS inhibition has been previously indicated (Iadecola 1993). Previously, we demonstrated that TAA administration resulted in a significant increase in the ADMA concentration in microdialysates of the prefrontal cortex, brain tissue homogenate and peripheral blood (Czarnecka *et al.* 2017, Milewski *et al.* 2015). Concentration of ADMA is higher in cerebellum and blood vessels than in other regions of the brain (Ueno *et al.* 1992), what may explain why in TAA rats L-arginine led to dilation of the MCAs and improved CBF more effectively in the cerebellum than in the prefrontal cortex. Large dilation of the MCAs compared to a slight CBF increase in the brain in response to L-arginine in TAA rats could be associated with L-arginine -related influence on the basal tone of cerebral blood vessels, which is greater in large arteries than arterioles (Faraci 1991). Therefore, regional differences in the cerebral response to L-arginine in control and TAA rats, observed in our study most likely resulted from variable vascularity pattern of the analyzed brain structures.

Our microdialysis study revealed that systemic administration of L-arginine at the dose of 200 mg/kg, in spite of a significant increase in brain L-arginine content did not affect extracellular ADMA within 160 min after injection. However, the same dose of L-arginine effectively increased cerebral perfusion both in the prefrontal cortex and cerebellum of TAA-treated rats, as well as in the prefrontal cortex of the control rats. Thus, it can be assumed that the beneficial effect of L-arginine administration was likely due to *de novo* NO synthesis predominantly by endothelial NOS, the most effective isoform synthesizing NO in the vasculature (Moncada and Higgs 2006). On the other hand, it cannot be excluded that the elevated ADMA level may aggravate the disturbances observed in the cerebral perfusion of ALF rats. The most likely scenario might be that ADMA, in combination with hypocapnia (Strauss 2007), increased intracranial pressure and hypotension (Filho *et al.* 2006), and, therefore, contributed to the decreased cerebral perfusion at this stage of disease. L-arginine is postulated as a therapy in vascular diseases accompanied by increased ADMA concentration (Czarnecka *et al.* 2017). However, it still remains an open question to what extent it is achievable to modulate pathologically increased ADMA, with the aim of improving the patients' condition. Importantly, our study demonstrates that beneficial effect of L-arginine on CBF was observed even under constantly raised ADMA level.

## Conclusion

The essential finding of the present study is that extraluminal L-arginine application evokes a pronounced vasodilation of the isolated MCAs from rats with ALF compared with control. The effect is most likely associated with limited availability of L-arginine caused by a high cerebral ADMA and glutamine concentrations accompanying ALF. The concomitantly reduced CBF in the cerebral cortex and cerebellum, partially reversed by the intraperitoneal administration of L-arginine, restored L-arginine/ADMA ratio and considerable reduction of glutamine concentration seem to confirm that disturbed nitrergic signaling plays a role in impaired cerebral perfusion during ALF.

Acknowledgement

The technical assistance of Mrs Inez Freśko and Krzysztof Milewski, PhD are gratefully acknowledged.

Funding

The author(s) disclosed receipt of the following financial support for the research, authorship, and/or publication of this article: this study was supported by Grant N 2013/09/B/NZ4/00536 from the National Science Centre. The equipment used for dimethylarginine and arginine determination was sponsored in part by the Centre for Preclinical Research and Technology (CePT), a project co-sponsored by European Regional Development Fund and Innovative Economy, The National Cohesion Strategy of Poland.

Declaration of conflict of interest

The author(s) declared no potential conflicts of interest with respect to the research, authorship, and/or publication of this article.

Authors' contributions

MZ sourced financial support; MZ and AC conceived and designed the experiments; AC performed experimental studies, statistical analysis and graphic processing of data; MA performed isolated cerebral artery studies and analyzed data; KJ performed MRI measurements and data analysis; RJ performed LC–DMS–MS/MS analysis; KK participated in MRI data acquisition; WH performed HPLC-FD analysis; AC and MZ wrote the manuscript.

References

Albrecht J., Hilgier W. and Rafałowska U. (1990) Activation of arginine metabolism to glutamate in rat brain synaptosomes in thioacetamide-induced hepatic encephalopathy: an adaptative response? *J. Neurosci. Res.* **25**, 125-130.

Albrecht J., Sidoryk-Węgrzynowicz M., Zielińska M. and Aschner M. (2010) Roles of glutamine in neurotransmission. *Neuron Glia Biol.* **6,** 263-276.

Albrecht J., Szeliga M. and Zielińska M. (2017) Brain glutamine. Roles in norm and pathology. In: Glutamine. Biochemistry, Physiology, and Clinical Applications. pp. 97-110. Edited by Dominique Meynial-Denis. ISBN 978-1-4822-3429-9. CRC Press,Taylor and Francis Group.

Aleksandrowicz M., Dworakowska B., Dolowy K. and Kozniewska E. (2017) Restoration of the response of the middle cerebral artery of the rat to acidosis in hyposmotic hyponatremia by the opener of large-conductance calcium sensitive potassium channels (BKCa). *J. Cereb. Blood Flow Metab.* **37,** 3219-3230.

Arnal J.F., Münzel T., Venema R.C., James N.L., Bai C.L., Mitch W.E. and Harrison D.G. (1995). Interactions between L-arginine and L-glutamine change endothelial NO production. An effect independent of NO synthase substrate availability. *J. Clin. Invest*. **95**, 2565-2572.

Becker V.U., Hansen H.C., Brewitt U. and Thie A. (1996) Visually evoked cerebral blood flow velocity changes in different states of brain dysfunction. *Stroke* **27,** 446-449.

Belle V., Kahler E., Waller C., Rommel E., Voll S., Hiller, K.-H., Bauer, W. R. and Haase, A. (1998) In Vivo quantitative mapping of cardiac perfusion in rats using a noninvasive MR spin-labeling method. *J. Magn. Reson. Imaging* **8,** 1240–1245.

Bode-Böger S.M., Scalera F. and Ignarro LJ. (2007) The L-arginine paradox: Importance of the L-arginine/asymmetrical dimethylarginine ratio. *Pharmacol. Ther*. **114,** 295-306.

Böger R.H. and Ron ES. (2005) L-Arginine improves vascular function by overcoming deleterious effects of ADMA, a novel cardiovascular risk factor. *Altern. Med. Rev.* **10,** 14-23.

Butterworth RF. (2003) Role of circulating neurotoxins in the pathogenesis of hepatic encephalopathy: potential for improvement following their removal by liver assist devices. *Liver Int.* **23,** 5–9.

Butterworth RF. (2013) The liver-brain axis in liver failure: neuroinflammation and encephalopathy. *Nat. Rev. Gastroenterol. Hepatol*. **10,** 522-528.

Cardounel A.J., Cui H., Samouilov A., Johnson W., Kearns P., Tsai A.L., Berka V. and Zweier J.L. (2007) Evidence for the pathophysiological role of endogenous methylarginines in regulation of endothelial NO production and vascular function. *J. Bio.l Chem.* **282,** 879–887.

Chen F.Y. and Lee TJ-F. (1995) Arginine synthesis from citrulline in perivascular nerves of cerebral artery. *J. Pharmacol. Exp. Ther.* **273,** 895–901.

Chen S., Li N., Deb-Chatterji M., Dong Q., Kielstein J.T., Weissenborn K. and Worthmann H. (2012) Asymmetric dimethyarginine as marker and mediator in ischemic stroke. *Int. J. Mol. Sci*. **13,** 15983-16004.

Cooper A.J.L. and Plum F. (1987) Biochemistry and physiology of brain ammonia. *Physiol. Rev.* **67,** 440–519.

Czarnecka A., Milewski K. and Zielińska M. (2017) Asymmetric Dimethylarginine and Hepatic Encephalopathy: Cause, Effect or Association? *Neurochem. Res*. **42,** 750-761.

Czarnecka A., Milewski K., Jaźwiec R. and Zielińska M. (2017) Intracerebral Administration of S-Adenosylhomocysteine or S-Adenosylmethionine Attenuates the Increases in the Cortical Extracellular Levels of Dimethylarginines Without Affecting cGMP Level in Rats with Acute Liver Failure. *Neurotox. Res.* **1,** 99-108.

Das A., Hoare M., Davies N., Lopes A.R., Dunn C., Kennedy P.T., Alexander G., Finney H., Lawson A., Plunkett F.J., Bertoletti A., Akbar A.N. and Maini M.K. (2008) Functional skewing of the global CD8 T cell population in chronic hepatitis B virus infection. *J. Exp. Med.* **205,** 2111–2124.

Durham S., Yonas H., Aggarwal S., Darby J. and Kramer D. (1995) Regional cerebral blood flow and CO2 reactivity in fulminant hepatic failure. *J. Cereb. Blood Flow Metab.* **15,** 329–335.

Faraci F.M. and Heistad D.D. (1990) Regulation of large cerebral arteries and cerebral microvascular pressure. *Circ. Res.* **66,** 8-17.

Faraci F.M. and Heistad D.D. (1992) Does basal production of nitric oxide contribute to regulation of brain-fluid balance? *Am. J. Physiol.* **262,** 340-344.

Faraci F.M., Brian J.E. Jr. and Heistad D.D. (1995) Response of cerebral blood vessels to an endogenous inhibitor of nitric oxide synthase. *Am. J. Physiol*. **269,** 1522-1527.

Faraci F.M. (1990) Role of nitric oxide in regulation of basilar artery tone in vivo. *Am. J. Physiol.* **259,** 1216-1221.

Faraci F.M. (1991) Role of endothelium-derived relaxing factor in cerebral circulation: large arteries vs. microcirculation. *Am. J. Physiol.* **261,** 1038-1042.

Felipo V. (2013) Hepatic encephalopathy: effects of liver failure on brain function. *Nat. Rev. Neurosci.* **14,** 851-858.

Filho J.A., Machado M.A., Nani R.S., Rocha J.P., Figueira E.R., Bacchella T., Rocha-e-Silva M., Auler J.O. Jr. and Machado M.C. (2006) Hypertonic saline solution increases cerebral perfusion pressure during clinical orthotopic liver transplantation for fulminant hepatic failure: preliminary results. *Clinics (Sao Paulo)* **61,** 231-238.

Filosa J.A., Morrison H.W., Iddings J.A., Du W. and Kim K.J. (2016) Beyond neurovascular coupling, role of astrocytes in the regulation of vascular tone. *Neuroscience* **323,** 96-109.

Harrison D.G. (1997) Cellular and molecular mechanisms of endothelial cell dysfunction. *J. Clin. Invest.* **100,** 2153-2157.

Hilgier W. and Olson J.E. (1994) Brain ion and amino acid contents during edema development in hepatic encephalopathy. *J. Neurochem.* **62,** 197-204.

Hilgier W., Olson J.E. and Albrecht J. (1996) Relation of taurine transport and brain edema in rats with simple hyperammonemia or liver failure. *J. Neurosci. Res.* **45,** 69-74.

Hilgier W., Freśko I., Klemenska E., Beresewicz A., Oja S.S., Saransaari P., Albrecht J. and Zielińska M. (2009) Glutamine inhibits ammonia-induced accumulation of cGMP in rat striatum limiting arginine supply for NO synthesis. *Neurobiol. Dis.* **35,** 75-81.

Hirata T., Kawaguchi T., Brusilow S.W., Traystman R.J. and Koehler R.C. (1999) Preserved hypocapnic pial arteriolar constriction during hyperammonemia by glutamine synthetase inhibition. *Am. J. Physiol. Heart Circ. Physiol*. **276,** 456–463.

Iadecola C. (1993) Regulation of the cerebral microcirculation during neural activity: is nitric oxide the missing link? *Trends in neurosciences* **16,** 206-214.

Iversen P., Sorensen M., Bak L.K., Waagepetersen H.S., Vafaee M.S., Borghammer P., Mouridsen K., Jensen S.B., Vilstrup H., Schousboe A., Ott P., Gjedde A. and Keiding S. (2009) Low cerebral oxygen consumption and blood flow in patients with cirrhosis and an acute episode of hepatic encephalopathy. *Gastroenterology* **136,** 863-871.

Iversen P., Mouridsen K., Hansen M.B., Jensen S.B., Sørensen M., Bak L.K., Waagepetersen H.S., Schousboe A., Ott P., Vilstrup H., Keiding S. and Gjedde A. (2014) Oxidative metabolism of astrocytes is not reduced in hepatic encephalopathy: a PET study with [(11)C]acetate in humans. *Front. Neurosci.* **8,** 353.

Jalan R., Olde Damink S.W., Hayes P.C., Deutz N.E. and Lee A. (2004) Pathogenesis of intracranial hypertension in acute liver failure: inflammation, ammonia and cerebral blood flow. *J. Hepatol*. **41,** 613-620.

Kajita Y., Takayasu M., Suzuki Y., Shibuya M., Mori M., Oyama H., Sugita K. and Hidaka H. (1995) Regional differences in cerebral vasomotor control by nitric oxide. *Brain Res. Bull.* **38,** 365-369.

Kawaguchi T., Brusilow S.W., Traystman R.J. and Koehler R.C. (2005) Glutamine-dependent inhibition of pial arteriolar dilation to acetylcholine with and without hyperammonemia in the rat. *Am. J. Physiol. Regul. Integr. Comp. Physiol.* **288,** 1612-1619.

Keynes R.G. and Garthwaite J. (2004) Nitric oxide and its role in ischaemic brain injury. *Curr. Mol. Med.* **4,** 179-191.

Kilpatrick I.C. (1991) Rapid, automated HPLC analysis of neuroactive and other amino acids in microdissected brain regions and brain slice superfusates using fluorimetric detection., pp. 555–578. In Neuroendocrine Research Methods (ed. Grenstein B.), Harwood Academic, London

Kimura M., Dietrich H.H. and Dacey R.G. Jr. (1994) Nitric oxide regulates cerebral arteriolar tone in rats. *Stroke* **25,** 2227-2233.

Kovách A.G., Szabó C., Benyó Z., Csáki C., Greenberg J.G., Reivich M. (1992) Effects of NG-nitro-L-arginine and L-arginine on regional cerebral blood flow in the cat. *J. Physiol.* **449,** 183–196.

Lee T.J.-F., Sarwinski S., Ishine T., Lai C.C. and Chen F.Y. (1996) Inhibition of cerebral neurogenic vasodilation by L-glutamine and nitric oxide synthase inhibitors and its reversal by Lcitrulline. *J. Pharmacol. Exp. Ther.* **276,** 353–358.

Liere V., Sandhu G. and DeMorrow S. (2017) Recent advances in hepatic encephalopathy. *F1000Res.* **6,** 1637.

Lundblad C. and Bentzer P. (2007) Effects of L-arginine on cerebral blood flow, microvascular permeability, number of perfused capillaries, and brain water content in the traumatized mouse brain. *Microvasc. Res.* **74,** 1-8.

Martens-Lobenhoffer J. and Bode-Böger SM. (2012) Quantification of l-arginine, asymmetric dimethylarginine and symmetric dimethylarginine in human plasma: a step improvement in precision by stable isotope dilution mass spectrometry. *J. Chromatogr. B. Analyt. Technol. Biomed. Life Sci.* **904,** 140–143.

Metea M.R. and Newman EA. (2006) Glial cells dilate and constrict blood vessels: a mechanism of neurovascular coupling. *J. Neurosci.* **26,** 2862–2870.

Milewski K., Hilgier W., Albrecht J. and Zielińska M. (2015) The dimethylarginine (ADMA)/nitric oxide pathway in the brain and periphery of rats with thioacetamide-induced acute liver failure: Modulation by histidine. *Neurochem. Int.* **88,** 26-31.

Milewski K. Rola dwumetyloargininn i mechanizmy regulujące ich stężenie w encefalopatii wątrobowej. PhD's Thesis, Mossakowski Medical Research Centre, Warsaw, Poland, 2017.

Moncada S. and Higgs E.A. (2006) The discovery of nitric oxide and its role in vascular biology. *Br. J. Pharmacol.* **147,** 193-201.

Morikawa E., Rosenblatt S. and Moskowitz M.A. (1992) L-arginine dilates rat pial arterioles by nitric oxide-dependent mechanisms and increases blood flow during focal cerebral ischaemia. *Br. J. Pharmacol.* **107,** 905-907.

Norenberg M.D. and Martinez-Hernandez A. (1979) Fine structural localization of glutamine synthetase in astrocytes of rat brain. *Brain Res*. **161**, 303-310.

Okada T., Watanabe Y., Brusilow S.W., Traystman R.J. and Koehler R.C. (2000) Interaction of glutamine and arginine on cerebrovascular reactivity to hypercapnia. *Am. J. Physiol. Heart Circ. Physiol.* **278,** 1577-1584.

Palenzuela L., Oria M., Romero-Giménez J., Garcia-Lezana T., Chavarria L. and Cordoba J. (2016) Gene expression profiling of brain cortex microvessels may support brain vasodilation in acute liver failure rat models. *Metab. Brain Dis.* **31,** 1405-1417.

Paxinos G. and Watson C. (1986) The rat brain in stereotaxic coordinates, 2nd edn. Academic Press, New York.

Rao V.L., Audet R.M. and Butterworth R.F. (1997) Portacaval shunting and hyperammonemia stimulate the uptake of L-[3H] arginine but not of L-[3H]nitroarginine into rat brain synaptosomes. *J. Neurochem.* **68,** 337-343.

Rosenblum W.I., Nishimura H. and Nelson G.H. (1990) Endothelium-dependent L-Arg- and L-NMMA-sensitive mechanisms regulate tone of brain microvessels. *Am. J. Physiol.* **259,** 1396-1401.

Rossitch E. Jr., Alexander E., Black P.M. and Cooke J.P. (1991) L-arginine normalizes endothelial function in cerebral vessels from hypercholesterolemic rabbits. *J. Clin. Invest.* **87,** 1295-1299.

Segarra G., Medina P., Ballester R.M., Lluch P., Aldasoro M., Vila J.M., Lluch S. and Pelligrino D.A. (1999) Effects of some guanidino compounds on human cerebral arteries. *Stroke* **30**, 2206-2210; discussion 2210-2211.

Sessa W.C., Hecker M., Mitchell J.A. and Vane J.R. (1990) The metabolism of L-arginine and its significance for the biosynthesis of endothelium-derived relaxing factor: L-glutamine inhibits the generation of L-arginine by cultured endothelial cells. *Proc. Natl. Acad. Sci. USA* **87,** 8607–8611.

Strauss GI. (2007) The effect of hyperventilation upon cerebral blood flow and metabolism in patients with fulminant hepatic failure. Dan. Med. Bull. **54,** 99-111.

Takahashi H., Koehler R.C., Hirata T., Brusilow S.W. and Traystman RJ. (1992) Restoration of cerebrovascular CO2 responsivity by glutamine synthesis inhibition in hyperammonemic rats. *Circ. Res.* **71,** 1220–1230.

Teerlink T., Luo Z., Palm F. and Wilcox CS (2009) Cellular ADMA: regulation and action. *Pharmacol. Res.* **60,** 448-460.

Tietge U.J., Bahr M.J., Manns M.P. and Boker K.H. (2002) Plasma amino acids in cirrhosis and after liver transplantation: influence of liver function, hepatic hemodynamics and circulating hormones. *Clin. Transplant.* **16,** 9–17.

Tsikas D., Böger R.H., Sandmann J., Bode-Böger S.M. and Frölich JC. (2000) Endogenous nitric oxide synthase inhibitors are responsible for the L-arginine paradox. *FEBS Lett.* **478,** 1-3.

Ueno S., Sano A., Kotani K., Kondoh K., Kakimoto Y. (1992) Distribution of free methylarginines in rat tissues and in the bovine brain. *J. Neurochem.* **59,** 2012-2016.

Willmot M., Gray L., Gibson C., Murphy S. and Bath P.M. (2005) A systematic review of nitric oxide donors and L-arginine in experimental stroke; effects on infarct size and cerebral blood flow. *Nitric Oxide* **12,** 141-149.

Yagnik G.P., Takahashi Y., Tsoulfas G., Reid K., Murase N. and Geller D.A. (2002) Blockade of the L-arginine/NO synthase pathway worsens hepatic apoptosis and liver transplant preservation injury. *Hepatology* **36,** 573–581.

Zheng G., Zhang L.J., Wang Z., Qi R.F., Shi D., Wang L., Fan X., Lu G.M. (2012) Changes in cerebral blood flow after transjugular intrahepatic portosystemic shunt can help predict the development of hepatic encephalopathy: an arterial spin labeling MR study. *Eur. J. Radiol.* **81,** 3851-3856.

Zielińska M., Ruszkiewicz J., Hilgier W., Fręśko I. and Albrecht J. (2011) Hyperammonemia increases the expression and activity of the glutamine/arginine transporter y+ LAT2 in rat cerebral cortex: implications for the nitric oxide/cGMP pathway. *Neurochem. Int.* **58,** 190-195.

Zielińska M., Skowrońska M., Fręśko I. and Albrecht J. (2012) Upregulation of the heteromeric $y^+$ LAT2 transporter contributes to ammonia-induced increase of arginine uptake in rat cerebral cortical astrocytes. *Neurochem. Int.* **61,** 531-535.

Zielińska M., Obara-Michlewska M., Hilgier W. and Albrecht J. (2014) Citrulline uptake in rat cerebral cortex slices: modulation by Thioacetamide -Induced hepatic failure. *Metab. Brain Dis.* **29**, 1053-1060.

Zielińska M., Milewski K., Skowrońska M., Gajos A. Ziemińska E., Beręsewicz A. and Albrecht J. (2015) Induction of inducible nitric oxide synthase expression in ammonia-exposed cultured astrocytes is coupled to increased arginine transport by upregulated y(+)LAT2 transporter. *J. Neurochem.* **135,** 1272-1281.

Zotti M., Schiavone S., Tricarico F., Colaianna M., D'Apolito O., Paglia G., Corso G. and Trabace L. (2008) Determination of dimethylarginine levels in rats using HILIC-MS/MS: an in vivo microdialysis study. *J. Sep. Sci.* **13,** 2511–2515.

Figure captions

Figure 1. Initial vessel diameter (a) Development of myogenic tone (b) and dilation in response to 20 mM KCl (c) of the isolated MCAs. All data are presented as the mean ± SEM; N = 5 for each group. **p<0.01 ***p<0.001 vs. Control; $^{\#}$p<0.05, $^{\#\#}$p<0.01, $^{\#\#\#}$p<0.001 vs. Control+$NH_4$; $^{\Delta\Delta}$p<0.01 vs. TAA+$NH_4$ group.

Figure 2. Response of the MCA to L-arginine (100 μM). Dilation is expressed as a percentage of maximum diameter. Data are expressed as the means ± S.E.M; N = 5 for each group except

N=4 for TAA+$NH_4$+ADMA 2 μM group. **p<0.01 vs. Control L-arg 100 μM; #p<0.05; ##p<0.01 vs. Control+$NH_4$ L-arg 100 μM.

Figure 3. The extracellular levels of ADMA (a) L-arginine (b) and L-arginine/ADMA ratio (c) in the prefrontal cortex of control and TAA rats: the effect of intraperitoneal administration of exogenous L-arginine (200 mg/kg). The results are presented as the mean ± SEM, N = 5 for each group for each time point. *p<0.05 vs. Control; # p<0.05, ### p<0.001 vs. TAA.

Figure 4. The extracellular levels of L-glutamine in the prefrontal cortex of control and TAA rats: the effect of intraperitoneal administration of exogenous L-arginine (200 mg/kg). The results are presented as the mean ± SEM, N = 5 for each group for each time point. ** p<0.01 vs. control basal level; ## p<0.01 vs. TAA basal level.

Figure 5. Slice location for perfusion measurement on sagittal and coronal brain images. Prefrontal cortex slice is marked in yellow, cerebellum slice is marked in red (a). Example of manually placed ROIs in prefrontal cortex (yellow line) and cerebellum (red line) used for calculation of average perfusion (b). Examples of perfusion maps obtained in prefrontal cortex (top row) and cerebellum (bottom row) for control (left) and TAA group (right) respectively. CBF map was calculated in ROI marked with yellow line on anatomic images (c). Quantitative data for CBF measurement before and after L-arginine administration in control and TAA rats in the prefrontal cortex (d) and cerebellum (e). All data are presented as the mean ± SEM; N = 6 for each group for each time point. * p<0.05 **p<0.01 vs. Control pre; # p<0.05, ## p<0.01 ### p<0.001 vs. TAA pre; Δp<0.05, ΔΔ p<0.01 vs. Control post.

**Data Reporting Checklist**

Animal studies based on ARRIVE guidelines (https://www.nc3rs.org.uk/arrive-guidelines)

*If any item is not applicable, indicate "n/a" and the reason why it is not applicable!*

| Checklist item | Description | Reported on page number |
|---|---|---|
| **Ethical statement** | - Institutional approval (name of institution and reference number) | - 5 |
| **Study design** | **Pre-registration of the study**<br>- Statement if/where study was pre-registered | - 5 |
| | **Randomization (mandatory for all animal experiments)**<br>- Full details of how animals were allocated to experimental groups<br>- Randomization method (randomization table, computer based randomization, etc.)<br>- Order in which animals were treated and assessed<br>- Statement if no randomization was performed | - 5 |
| | **Blinding**<br>- Who was blinded (experimenter, person assigning subjects to groups, etc.)<br>- When (at which point in the experimental course)<br>- How (describe blinding procedure)<br>- Statement if no blinding was performed | - 7 |
| | **Predetermined sample size calculation (mandatory for animal studies)**<br>- Statement whether statistical methods were used to predetermine sample size and description of the calculation | - 5 |
| | **Outcomes**<br>- Pre-specified primary or secondary endpoint, otherwise exploratory<br>- Predefined criteria how to deal with outliers | - 10 |
| | **Provide time-line diagram or flow-chart (mandatory for animal experiments)** | - 5, in text |
| | **At the end of study report**<br>- Information on replication [*biological* (independent data points from different sources) or *technical replicates* (repetition of the assay/sample preparation from the same source)]<br>- Definition of Sample size (n): Report exact numbers for all experiments (figures)<br>- Explanation of any sample size differences between beginning and end for each experiment | - 10<br>- 5, 26-27 Figures legend<br>- 6, 10 |
| | **Data availability**<br>- Mandatory for: Protein, DNA and RNA sequences, Macromolecular structures, crystallographic data for small molecules, microarray data (*strongly recommended for all other data sets*) | - n/a<br>- at the institutional |

| Checklist item | Description | Reported on page number |
|---|---|---|
| | - Weblink to repository / accession codes / other unique identifiers | repository |
| | - Computer code availability | - n/a |
| | - Statement to any restrictions on the availability of materials/data | password security |
| | - Raw western blot or electrophoresis images provided as supplement material? (Yes/No) | - No |
| **Experimental procedure** | **Precise details of all procedures carried out:** | |
| | - What (Materials such as antibodies, reagents with Research Resource Identifiers ((RRIDs) from https://scicrunch.org) | |
| | - Antibodies: validation data available from the company or conducted by the authors | - n/a |
| | - How (drug formulation; dose, site and route, anesthesia/analgesia, surgical procedure, method of euthanasia, details about specialist equipment incl. suppliers) | - 5-10 |
| | - When (e.g. time of day). | |
| | - Where (e.g. home cage, laboratory, water maze). | |
| | - Why (e.g. rationale for choice of specific anesthetic, route of administration, drug dose used) | - 5-10 |
| **Animals/ Cell lines** | - Species, strain | - 5 |
| | - Source of animals / cell lines (indicate provider, catalog number, RRID from https://scicrunch.org) | - 5 n/a |
| | - State if and when animals or cell lines were last authenticated | - n/a |
| | - Statement if cell line is listed as a commonly misidentified cell line by the International Cell Line Authentication Committee (ICLAC; http://iclac.org/databases/cross-contaminations/) | - n/a |
| | o If the cell line is listed, provide a scientific justification to use this cell line | - 5 |
| | - Sex | - 5 |
| | - Age | - 5 |
| | - Weight | - 5 |
| | - Housing (type of cage, number of cage companions) | - 5 |
| | - Husbandry (access to food and water, light/dark cycle, temperature, environmental enrichment) | |
| | - Welfare-related assessments and interventions | - 5 |
| **Reporting statistics** | **Describe the statistical tests that were used and why these tests were chosen** | - 10-12 |
| | - Details of the statistical methods used for each analysis | |
| | - Specify the unit of analysis (n) for each dataset (e.g. single animal, group of animals, single neuron) | |
| | - Describe any methods used to | |
| | o assess whether the data met the assumptions of the statistical approach | |
| | o to control for confounding | |
| | o examine subgroups and interactions | |
| | - Explain how missing data were addressed | |
| | - Provide exact p-values | |
| | - Correction for risk of false positives in case of multiple testing | |

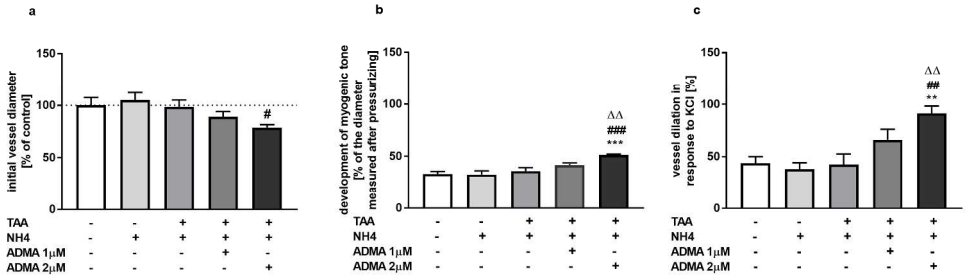


Figure 1. Initial vessel diameter (a) Development of myogenic tone (b) and dilation in response to 20 mM KCl (c) of the isolated MCAs. All data are presented as the mean ± SEM; N = 5 for each group. **p<0.01 ***p<0.001 vs. Control; #p<0.05, ##p<0.01, ###p<0.001 vs. Control+$NH_4$; ΔΔp<0.01 vs. TAA+$NH_4$ group.

250x80mm (300 x 300 DPI)

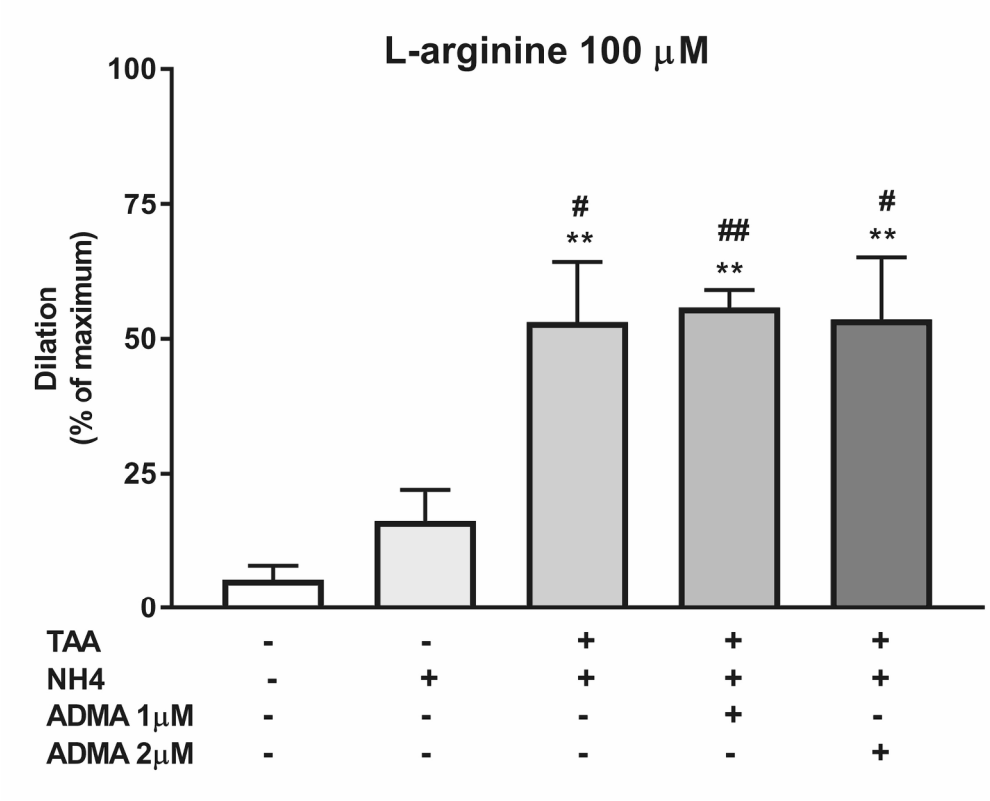


Figure 2. Response of the MCA to L-arginine (100 μM). Dilation is expressed as a percentage of maximum diameter. Data are expressed as the means ± S.E.M; N = 5 for each group except N=4 for TAA+$NH_4$+ADMA 2 μM group. **p<0.01 vs. Control L-arg 100 μM; #p<0.05; ##p<0.01 vs. Control+$NH_4$ L-arg 100 μM.

103x83mm (600 x 600 DPI)

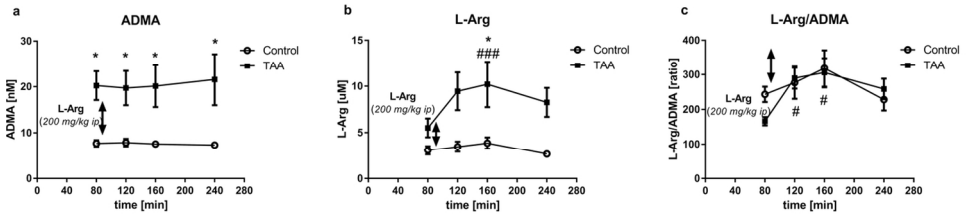


Figure 3. The extracellular levels of ADMA (a) L-arginine (b) and L-arginine/ADMA ratio (c) in the prefrontal cortex of control and TAA rats: the effect of intraperitoneal administration of exogenous L-arginine (200 mg/kg). The results are presented as the mean ± SEM, N = 5 for each group for each time point. *p<0.05 vs. Control; # p<0.05, ### p<0.001 vs. TAA.

63x16mm (600 x 600 DPI)

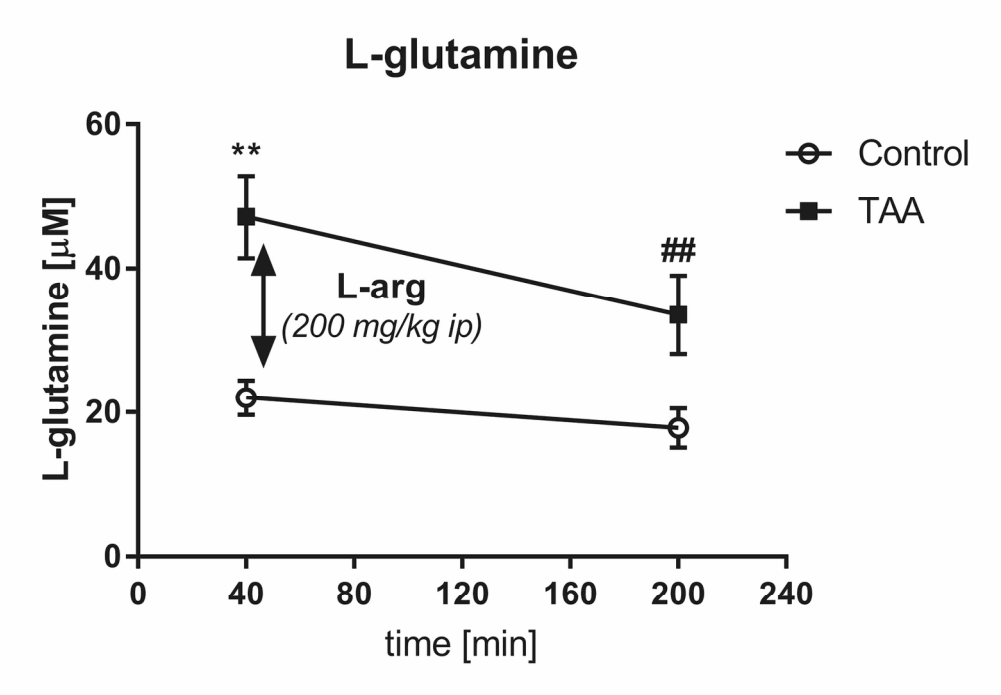


Figure 4. The extracellular levels of L-glutamine in the prefrontal cortex of control and TAA rats: the effect of intraperitoneal administration of exogenous L-arginine (200 mg/kg). The results are presented as the mean ± SEM, N = 5 for each group for each time point. ** p<0.01 vs. control basal level; ## p<0.01 vs. TAA basal level

81x56mm (600 x 600 DPI)

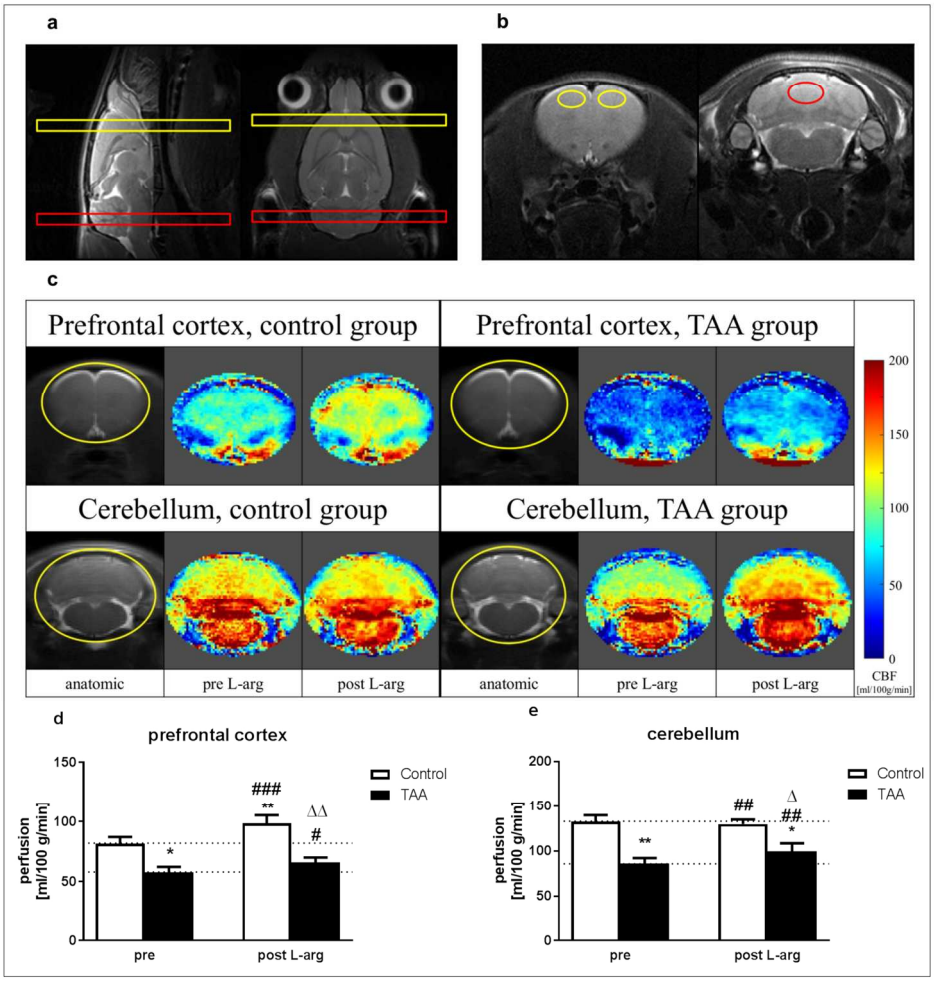


Figure 5. Slice location for perfusion measurement on sagittal and coronal brain images. Prefrontal cortex slice is marked in yellow, cerebellum slice is marked in red (a). Example of manually placed ROIs in prefrontal cortex (yellow line) and cerebellum (red line) used for calculation of average perfusion (b). Examples of perfusion maps obtained in prefrontal cortex (top row) and cerebellum (bottom row) for control (left) and TAA group (right) respectively. CBF map was calculated in ROI marked with yellow line on anatomic images (c). Quantitative data for CBF measurement before and after L-arginine administration in control and TAA rats in the prefrontal cortex (d) and cerebellum (e). All data are presented as the mean ± SEM; N = 6 for each group for each time point. * p<0.05 **p<0.01 vs. Control pre; # p<0.05, ## p<0.01 ### p<0.001 vs. TAA pre; Δp<0.05, ΔΔ p<0.01 vs. Control post.

180x185mm (300 x 300 DPI)